A multiscale description of particle composites: from lattice microstructures to micropolar continua

Patrizia Trovalusci[a,*], Maria Laura De Bellis[b], Renato Masiani[a]

[a]*Department of Structural and Geotechnical Engineering, Sapienza University of Rome*
[b]*Department of Innovation Engineering, University of Salento, Lecce, Italy*

Abstract

We present a two–steps multiscale procedure suitable to describe the constitutive behavior of hierarchically structured particle composites. The complex material is investigated considering three nested scales, each one provided by a characteristic length. At the lowest scale (micro), a periodic lattice system describes in detail the mechanical response governed by interactions between rigid grains connected through elastic interfaces. At the intermediate scale (meso), the material is perceived as heterogeneous and characterized by deformable particles randomly distributed into a base matrix, either stiffer or softer. At the macroscopic scale, the material is represented as a micropolar continuum. The micro/meso transition is governed by an energy equivalence procedure, based on a generalized Cauchy–Born correspondence map between the discrete degrees of freedom and the continuum kinematic fields. The meso/macro equivalence exploits a statistically–based homogenization procedure, allowing us to estimate the equivalent micropolar elastic moduli. A numerical example illustrating the integrated multiscale procedure complements the paper.

Keywords: Random composites, multiscale procedures, micropolar continua, lattice microstructures.

June 16, 2017

1. Introduction. A three–levels procedure: basics

The mechanical behavior of complex materials, characterized at finer scales by the presence of heterogeneities of significant size and texture, strongly depends on their microstructural features. By lacking in internal scale parameters, the classical continuum does not always seem appropriate to describe the macroscopic behavior of these materials when it is important to take into account, besides the disposition, the size and orientation of the micro heterogeneities.

*Corresponding author
Email address: patrizia.trovalusci@uniroma1.it (Patrizia Trovalusci)

In the modeling of materials with microstructure such as particle composites in particular, the discontinuous and heterogeneous nature of the material must be taken into account, because interfaces and/or material phases dominate the gross mechanical behavior [1]. This calls for the need of non–classical and non–local continuum descriptions that can be obtained through multi–scale approaches aimed at deducing properties and relations by bridging information at proper underlying sub–levels via energy equivalence criteria, as widely acknowledged in literature [2, 3, 4, 5, 6, 7, 8, 9, 10, 11, 12, 13, 14, 15, 16, 17, 18]. By adopting such approaches it is possible to preserve memory of the microstructure, and in particular of the presence of material length scales, without resorting to the discrete modeling, that can be often cumbersome.

In the framework of a multi–scale modeling aiming at deriving homogeneous anisotropic continua suitable for coarsely represent the microstructure, the non–local character of the description is crucial [19, 20, 21]. In particular, this occurs in problems in which a characteristic internal length, l, is comparable to the macroscopic (structural) length, L [22, 20]. Among non–local theories, it is useful to distinguish between 'explicit' or 'strong' and 'implicit' or 'weak' non–locality [23, 24, 25], where the so–called implicit non–locality concerns continua with extra degrees of freedom such as in the micropolar continuum formulations [26, 27, 28, 29, 30] adopted herein. Basing on the proved effectiveness of the micropolar continuum modeling for periodic media over years [3, 10, 14, 31, 32, 16], the micropolar multiscale modeling has been here extended for deriving constitutive models of random media such as ceramic/metal/polymer matrix composites, i.e. polycrystals with interfaces (grain boundaries or thin/thick interfaces), or short fiber-reinforced composites, or even masonry–like materials (Roman concrete, rocks) that frequently exhibit random microstructure. For these materials a two-step multi-scale procedure has been developed. At the microscopic level the material is described as a lattice system, at a mesoscopic level as a two–phase micropolar continuum and at the macroscopic level as a homogeneous micropolar continuum (Figure 1). The resulting continuum at the highest level is, thus, dependent on the hierarchy of three characteristic lengths, namely: the structural size at the macroscopic level, L_M; a typical size, L, at the mesoscopic level, related to the size d of the heterogeneities; the intrinsic material length, l_μ, at the microscopic level.

For the transition from the discrete micro–level to the two–phases continuum meso–level (i), a coarse–graining procedure based on a generalized Cauchy–Born correspondence maps and energy equivalence has been adopted [10, 13, 16]. For the meso/macro level transition instead (ii), a statistical homogenization procedure has been developed [33, 34]. This procedure is based on the solution of Boundary Value Problems (BVPs), posed on Statistically Representative Elements (SVEs), under Boundary Conditions (BCs) derived from a generalized macrohomogeneity condition of Hill's type [35]. Through hierarchies of bounds for the elastic moduli, the result is the estimation of the size of the Representative Volume Element (RVE) to adopt for performing homogenization. In this framework, a new criterion of convergence has been introduced and the elastic, classical and micropolar,

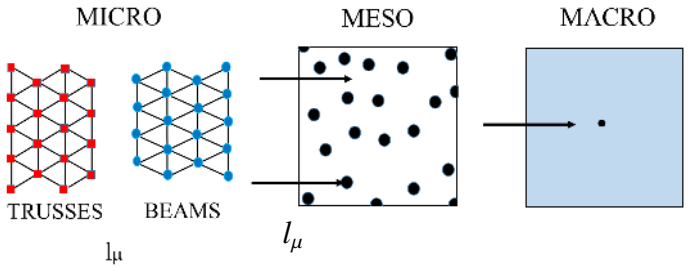

Figure 1: Schematic of the three scales homogenization procedure. Lattice system (micromodel); two-phases continuum (mesomodel); homogenized continuum (macromodel).

constitutive moduli have been identified for particular classes of particle composites.

As an example of material to which apply such a multiscale approach, we consider a special case of particulate composite: the ceramic matrix composites (CMCs), comprising micro– or nano–scale metallic particles in a ceramic matrix. In these materials the particles are discrete and they typically provide a toughening increment by plastically deforming and preventing the advance of cracks. Among others, we consider Alumina–Zirconia CMC of Figure 2, where the SEM images show different assemblies ranging from pure Alumina to pure Zirconia. These CMCs are very promising as structural materials, combining the properties of the Alumina matrix (high hardness and Young's modulus) with additional toughening effects, due to the Zirconia dispersion, see [36]. At the microscopic scale the material exhibits a complex microstructure pertaining both to matrix and inclusions that appear as spatial assemblies of irregular particles seamlessly arranged, as reported in Figure 3a, where a sketch of the micro–structure is shown. A schematic of the meso and micro levels for the aforementioned $Al_2O_3 - ZrO_2$ CMC composite is presented in Figure 3b.

The content of the paper is resumed in the following.
Section 2 - step (i). We begin with illustrating the discrete–continuum approach adopted to perform the micro/meso transition. Considering the reference material made of particles embedded in a matrix, with different material properties, we assume that each constituent is a material with microstructure that can be described as a lattice system. At the underlying micro–level, due to the high volume fraction of particles (grains) composing each constituent (Figure 2, 3b), the microstructure of both materials is considered deterministic.

Thus, we focus on physically–based discrete–continuous models, as originated by the molecular models of Nineteenth century to give explanations 'per causas' of elasticity [38, 39]. In particular, a discrete–continuum deterministic approach – based on a generalization of the so-called Cauchy–Born rule currently used in crystal elasticity as well in the classical molecular theory of elasticity [40] – is used for deriving a continuum equivalent in terms of energy to lattice models made of interacting particles, inside which no–forces are accounted for [19]. These interactions can be represented by central forces along the line connecting

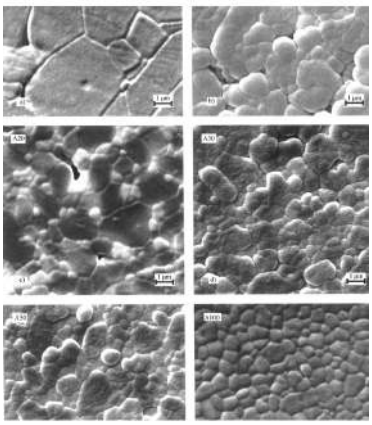

Figure 2: SEM images of different types of Alumina matrix Al_2O_3 and Zirconia ZrO_2 inclusions composites, ranging from pure Alumina (first) to pure Zirconia (last), [37].

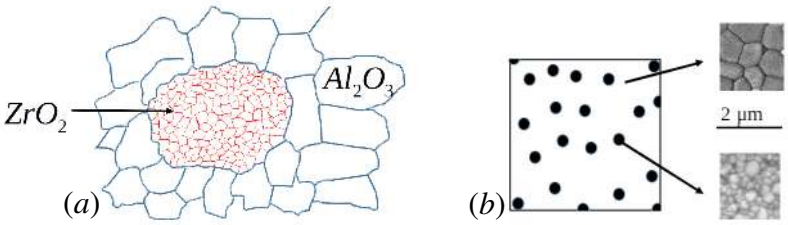

Figure 3: a) Sketch of Alumina-Zirconia Ceramic Matrix Composite. b) Meso and Micro scales of $Al_2O_3 - ZrO_2$ CMC composite.

the particle centers or by forces and couples, and in this sense the discrete system can be, respectively, reconnected to truss–like or beam–like networks [41, 32, 42], or even to other kind of 'structured' lattice systems, as in [9, 13]. The derived equivalent continuum retains memory of the fine organization of the material by means of additional field descriptors and it is named multifield continuum.

Once defined the lattice system, basing on such a generalized rule and assuming proper response functions for the lattice interactions, the requirement of the preservation of the strain energy in the micro/meso transition, for any admissible deformation field over a REV, allow us to identify the (classical and non-classical) constitutive parameters of the mesomodel, in terms of the geometry of the microstructure (shape, size, orientation, texture).

The meso–scale model is then obtained as the result of such a discrete–continuum, coarse–graining, procedure, that in the case of a truss–like scheme leads to a classical continuum, while in the case of a beam–like scheme generates a multifield continuum with rigid local structure (micropolar). The latter case is here considered, since in the case of polycrystals with thin interfaces (Figure 2) the microscopic bending deformation mechanisms are expected to be predominant. Although it is not trivial, the procedure can be extended to fiber–beam networks, representing fiber reinforced composites or cellular materials, or other kind of ceramic/metal matrix composites, up to concrete, masonry–like and geo–materials, for which micro–bending has also a significant role.

Section 3 - step (ii). The second step of the multiscale procedure concerns the transition from a micropolar two–phases continuum to a micropolar homogeneous continum through an average–field homogenization procedure. This procedure is based on the solution of BVPs, defined at the meso–level, under Dirichlet and Neumann BCs derived from a macrohomogeneity condition of Hill's type, here generalized in order to take into account the additional degrees of freedom of the micropolar continuum, namely the relative rotation and curvature [35].

Due to the generally low volume fraction at the meso–level, the material is perceived as a random aggregate of inclusions embedded in a matrix [43], either softer or stiffer. As a result of the coarse–graining procedure (i), both the inclusions and the matrix are described as isotropic micropolar continua. The macroscopic continuum is also supposed to be micropolar, able to naturally account for scale and skew–symmetric shear effects [10, 16]. In this framework, the adopted generalized macrohomogeneity condition ensures a one–to–one correspondence between the two scales, avoiding the introduction of kind of internal constraints for the deformation mechanisms, as occurs in the case of continua of different type [2, 14].

With the aim of investigating the gross mechanical response of this special class of random composites, we adopt a statistically–based multiscale procedure which allow us to detect the size of the RVE, that is unknown in the case of random media [44, 45], and to estimate the constitutive moduli of the energy equivalent homogeneous micropolar con-

tinuum [33, 34]. The RVE is obtained by increasing a scale factor representing the ratio between the size of a control window (SVE) and the particle size, until the statistical convergence, defined through an ad hoc conceived criterion, is reached.

Section 4. Some results obtained for an ideal material that mimics the internal micro/meso structure of a CMC material are presented. Two material case studies, with inclusions either stiffer or softer than the matrix, are compared. These examples, representative of different kind of composites – ranging from metal or ceramic matrix composites up to concrete or masonry–like materials – highlight the possibility to detect the constitutive parameters at the three scales of description, starting from the knowledge of the geometry and the material parameters of the internal structure at the discrete micro–level. The effect of the randomness of the spatial distribution of inclusions at the meso–level in identifying the shear and bending moduli of the equivalent homogeneous micropolar continuum is also taken into account. We consider this three–level homogenization procedure to be promising for grossly describing the material non–linear behavior starting from the accurate description of damaging and/or fracture phenomena, that often onset at the level of microscopic interfaces [46, 47].

2. Micro/Meso transition (ii) - Coarse–graining

At the first level – the finest one, conventionally defined as micro–level – the reference material (Figure 3) is described as a lattice system made of rigid particles of hexagonal shape and elastic interfaces (Figure 4).

Since many years it has been shown that in such systems the gross mechanical behavior is strongly influenced by the particle size and orientation and that this microstructural feature can be properly taken into account by identifying continua of the Cosserat type [48, 49, 50, 3] Here below we adopt the procedure described in [51], and then extended and generalized in [10, 16], for deriving a micropolar continuous model energy equivalent to a lattice system made of particles interacting through forces and couples, as in a beam–like network [41]. The micropolar continuum is identified by assuming the conservation of the power expended in the transition from the micro (discrete) to the meso (continuous) model, for a given class of regular motions. The constitutive functions for the meso–level continuous materials are then derived in terms of the geometrical and mechanical properties of the rigid particles and interfaces. Particular attention is devoted to the evaluation of the characteristic intrinsic length, l_μ, of each micropolar constituent as directly gathered by the underlying microstructure. These parameters, adopted in the constitutive law at the mesoscopic level, are, indeed, difficult to estimate through experimental tests [52] and the calibration of their values is a very debated issue.

2.1. Lattice system

In this paragraph the methodological aspects of the procedure are developed within the framework of linearized elasticity, where velocity and angular velocity stand for infinitesimal displacement and rotations, respectively. It is worth noting, however, that the procedure can be employed in more general contexts, even if the generalization is not trivial.

Let us assume that each particle, $\mathcal{A}$, is a rigid body. The vector $\mathbf{w}^a$ and the skew-symmetric tensor $\mathbf{W}^a$ ($\mathbf{W}^a = -(\mathbf{W}^a)^T$) respectively denote the velocity of the particle center, g^a, and the particle angular velocity.

Under the rigid body assumption, for any point belonging to the particle $(\cdot)$, it is:

$$\begin{aligned} \mathbf{w}^a(\cdot) &= \mathbf{w}^a + \mathbf{W}^a((\cdot) - g^a)\,, \\ \mathbf{W}^a(\cdot) &= \mathbf{W}^a\,. \end{aligned} \tag{1}$$

Let $\mathcal{A}$ and $\mathcal{B}$ be two interacting rigid particles and select a pair of points ($p^a \in \mathcal{A}$, $p^b \in \mathcal{B}$), along the interface between $\mathcal{A}$ and $\mathcal{B}$, that we call a 'test pair'. As strain measures for the test pair (p^a, p^b) we then assume the following quantities:

$$\begin{aligned} \mathbf{w}_p &= \mathbf{w}^a(p^a) - \mathbf{w}^b(p^b)\,, \\ \mathbf{W}_p &= \mathbf{W}^a(\cdot) - \mathbf{W}^b(\cdot)\,, \end{aligned} \tag{2}$$

that, using Equations (1), can be rewritten as follows:

$$\begin{aligned} \mathbf{w}_p &= \mathbf{w}^a - \mathbf{w}^b + \mathbf{W}^a(p^a - g^a) - \mathbf{W}^b(p^b - g^b)\,, \\ \mathbf{W}_p &= \mathbf{W}^a - \mathbf{W}^b\,. \end{aligned} \tag{3}$$

Furthermore, we assume that the contact interaction between the two particles $\mathcal{A}$ and $\mathcal{B}$ is described by a force and a couple through the test pair (p^a, p^b). The vector $\mathbf{t}^a$ ($\mathbf{t}^b$) and the skew-symmetric tensor $\mathbf{C}^a$ ($\mathbf{C}^b$) respectively represent the force and the couple that $\mathcal{B}$ ($\mathcal{A}$) exerts on $\mathcal{A}$ ($\mathcal{B}$).

Let us consider now a reference portion $\mathcal{M}$ of the system of particles made of n particles of total volume V, defined as the sum of the elementary volumes pertaining to the particles. The power of the internal actions acting on $\mathcal{M}$ can be expressed in the form:

$$\pi = \sum_i (\mathbf{t}^i \cdot \mathbf{w}^i + \frac{1}{2}\mathbf{C}^i \cdot \mathbf{W}^i)\,, \tag{4}$$

with i ranging from 1 to n. By taking into account the balance equations for each p^{th} test pair:

$$\begin{aligned} \mathbf{t}^a + \mathbf{t}^b &= \mathbf{0} \\ \mathbf{C}^a + \mathbf{C}^b - \frac{1}{2}\{[(p^a - p^b) \otimes \mathbf{t}^a - \mathbf{t}^a \otimes (p^a - p^b)]\} &= \mathbf{0}\,, \end{aligned} \tag{5}$$

the following mean power formula over $\mathcal{M}$ can be derived in the form:

$$\pi = \frac{1}{V}\sum_p \pi_p, \qquad \pi_p = \mathbf{t}_p \cdot [\mathbf{w}_p - \mathbf{W}^a(p^a - p^b)] + \frac{1}{2}\mathbf{C}_p \cdot \mathbf{W}_p\,, \tag{6}$$

where $\mathbf{t}_p = \mathbf{t}_a = -\mathbf{t}^b$ and $\mathbf{C}_p = \mathbf{C}^a = -\mathbf{C}^b + \frac{1}{2}\{[(p^a - p^b) \otimes \mathbf{t}^b - \mathbf{t}^b \otimes (p^a - p^b)]\}$, and where the range of p being the number of the test pairs in $\mathcal{P}$.

We finally assume the following linear constitutive functions for each test-pair in $\mathcal{M}$:

$$\begin{aligned} \mathbf{t}_p &= \mathbf{K}_p \mathbf{w}_p\,, \\ \mathbf{C}_p &= \mathbb{K}_p \mathbf{W}_p\,, \end{aligned} \tag{7}$$

where the elastic second order tensor $\mathbf{K}_p$ and the fourth order tensor $\mathbb{K}_p$ have as components the normal, tangential and rotational stiffness at the p^{th} interface.

2.2. Identification of the micropolar continuum

Let us consider a continuum body occupying the region $\mathcal{B}$, a place $x \in \mathcal{B}$, and an open neighborhood, $\mathcal{P}$, of x. The deformation of any point $p \in \mathcal{P}$ is assumed to be homogeneous and approximated by the functions:

$$\begin{aligned} \mathbf{w}(p) &= \mathbf{w}(x) + \mathbf{H}(x)(p - x) \\ \mathbf{W}(p) &= \mathbf{W}(x) + \mathbb{H}(x)(p - x)\,, \end{aligned} \tag{8}$$

with $\mathbf{H} = \partial \mathbf{w}(x)/\partial x$ and $\mathbb{H} = \partial \mathbf{W}(x)/\partial x$.Equation (8) is a generalization of the Cauchy–Born rule, [38].

If we assume that the lattice system has a modular structure, the deformation of the lattice representative element $\mathcal{M}$ (*module*) can be related to the deformation of $\mathcal{P}$ by postulating that:

$$\begin{aligned} \mathbf{w}^a &= \mathbf{w}(x) + \mathbf{H}(x)(g^a - x) \\ \mathbf{W}^a &= \mathbf{W}(x) + \mathbb{H}(x)(g^a - x) \end{aligned} \tag{9}$$

Finally, by using Equations (8) and (9), the expressions (3) can be rewritten as:

$$\begin{aligned} \mathbf{w}_p &= \mathbf{H}(x)(g^a - g^b) - \mathbf{W}(x)(g^a - g^b) \\ &\quad +[\mathbb{H}(x)(g^a - x)](p^a - g^a) - [\mathbb{H}(x)(g^b - x)](p^b - g^b)\,, \\ \mathbf{W}_p &= \mathbb{H}(x)(g^a - g^b)\,. \end{aligned} \tag{10}$$

Using the deformation correspondence proposed above (9), it is then possible to obtain an expression of the power of the contact actions in the discrete model in terms of the kinematic quantities pertaining to the continuum ones. With regard to a generic test pair

(p^a, p^b), from (6) and using Equations (10), we obtain the test–pair power as function of continuous kinematic fields $\mathbf{H}(x)$, $\mathbf{W}(x)$, $\mathbb{H}(x)$:

$$\begin{aligned}\pi_p &= \mathbf{t}_p \cdot \{[\mathbf{H}(x) - \mathbf{W}(x)](g^a - g^b) \\ &\quad +[\mathbb{H}(x)(g^a - x)](p^a - g^a) - [\mathbb{H}(x)(g^b - x)](p^b - g^b)\} \\ &\quad +\frac{1}{2}\,\mathbf{C}_p \cdot \mathbb{H}(x)(g^a - g^b)\,. \end{aligned} \tag{11}$$

By performing simple algebra, the above expression can be rewritten in the form:

$$\begin{aligned}\pi_p &= (\mathbf{H} - \mathbf{W}) \cdot \left[\mathbf{t}_p \otimes (g^a - g^b)\right] \\ &\quad +\frac{1}{2}\,\mathbb{H} \cdot \left\{2\mathbf{t}_p \otimes [(p^a - g^a) \otimes (g^a - x) - (p^b - g^b) \otimes (g^b - x)]\right. \\ &\quad \left. + \mathbf{C}_p \otimes (g^a - g^b)\right\}\,. \end{aligned} \tag{12}$$

where the dependence on x of the kinematic fields has been understood.

The constitutive functions for the contact actions of the equivalent continuum can thus be obtained by requiring that the mean power of the lattice system over the module, expressed as function of the strain fields $(\mathbf{H} - \mathbf{W})$, $\mathbf{W}$, equals the stress power density at x in such a way that:

$$\begin{aligned}\overline{\pi}[(\mathbf{H} - \mathbf{W}),\, \mathbb{H}] &= \frac{1}{V}\sum_p \pi_p[(\mathbf{H} - \mathbf{W}),\, \mathbb{H}] \\ &= (\mathbf{H} - \mathbf{W}) \cdot \mathbf{S} + \frac{1}{2}\mathbb{S} \cdot \mathbb{H}\,, \quad \forall\, (\mathbf{H} - \mathbf{W}),\, \mathbb{H}\,, \end{aligned} \tag{13}$$

where $\mathbf{S}$ and $\mathbb{S}$ are the stress measures of the micropolar continuum power conjugated to $(\mathbf{H} - \mathbf{W})$ and $\mathbf{W}$, respectively.

In Equation (13) V denotes the volume of $\mathcal{M}$, supposed as centered at x, and the summation is extended to all the 'test pairs' appearing in the selected module $\mathcal{M}$. Enforcing this equivalence and taking into account Equations (12), (7) and (10) again, we have:

$$\begin{aligned}\mathbf{S} &= \frac{1}{V}\sum_p \mathbf{t}_p \otimes (g^a - g^b) \\ \mathbb{S} &= \frac{1}{V}\sum_p \{\, 2\,\mathbf{t}_p \otimes [(p^a - g^a) \otimes (g^a - x) - (p^b - g^b) \otimes (g^b - x)] \\ &\quad +\mathbf{C}_p \otimes (g^a - g^b)\,\} \end{aligned} \tag{14}$$

with

$$\begin{aligned}\mathbf{t}_p &= \mathbf{K}_p\,\{\,(\mathbf{H} - \mathbf{W})(g^a - g^b) \\ &\quad +[\mathbb{H}(g^a - x)](p^a - g^a) - [\mathbb{H}(g^b - x)](p^b - g^b)\,\} \\ \mathbf{C}_p &= \mathbb{K}_p\,[\mathbb{H}(g^a - g^b)] \end{aligned} \tag{15}$$

3. Meso/Macro transition (ii) - Homogenization

As a result of the coarse–graining procedure presented in Section 2, both the inclusions and the matrix are described as micropolar continua which deterministic structure is encoded in the power density formula (13). The macroscopic continuum is also supposed to be micropolar, which in the case of periodic media have been proved to be able to naturally account for scale and skew-symmetric shear effects [16].

At the meso–level the kind of composites here considered (Figure 3) has particles embedded in a matrix, randomly distributed according to a so-called dilute concentration (low volume fraction of max 40%) and they cannot be treated as periodic. The transition from the mesoscopic to the macroscopic scale is then performed resorting to a statistical homogenization approach applied to a material with randomly distributed inclusions, either stiffer or softer than the matrix. The procedure, set at the meso–level, is based on the solution of BVPs consistent with a generalized macrohomogeneity condition of Hills type [33].

3.1. The micropolar model

In the context of the linearized theory, each material point is characterized by the velocity vector $\mathbf{w}$ and the angular velocity skew–symmetric tensor $\mathbf{W}$. The strains measures are the strain, $\mathbf{U}$, and curvature, $\mathbb{U}$, tensor, which are defined according to the compatibility equations:

$$\begin{aligned} \mathbf{U} &= \mathbf{H} - \mathbf{W} = \mathbf{E} + \boldsymbol{\Theta} - \mathbf{W}\,, \\ \mathbb{U} &= \mathbb{H}\,, \end{aligned} \tag{16}$$

where $\mathbf{E} = (\mathbf{H} + \mathbf{H}^T)/2$ and $\boldsymbol{\Theta} = (\mathbf{H} - \mathbf{H}^T)/2$, respectively, are the symmetric and the skew-symmetric part of $\mathbf{H} = \partial\mathbf{w}/\partial x$ and $\mathbb{H} = \partial\mathbf{W}/\partial x$.

The power conjugated stress measures, respectively, are: the stress tensor $\mathbf{S}$ and the couple stress tensor $\mathbb{S}$. If we decompose the stress tensor into its symmetric, $\mathbf{T} = (\mathbf{S}+\mathbf{S}^T)/2$, and skew-symmetric, $\mathbf{A} = (\mathbf{S} - \mathbf{S}^T)/2$, part, $\mathbf{S} = \mathbf{T} + \mathbf{A}$, the stress density formula of the micropolar continuum can be written:

$$\pi = \mathbf{S} \cdot \mathbf{U} + \frac{1}{2}\,\mathbb{S} \cdot \mathbb{U} \;= \mathbf{T} \cdot \mathbf{E} + \mathbf{A} \cdot (\boldsymbol{\Theta} - \mathbf{W}) + \frac{1}{2}\,\mathbb{S} \cdot \mathbb{U} \tag{17}$$

The balance equations for the continuum, occupying an Euclidean region $\mathcal{B}$, with no external body forces and couples, can be then derived from a generalized formulation of the virtual power theorem as:

$$\begin{aligned} div\,\mathbf{S} &= \mathbf{0}\,, \\ div\,\mathbb{S} + 2\mathbf{A} &= 0\,, \end{aligned} \tag{18}$$

while, accounting for a generalized version of the Cauchy theorem, the boundary conditions on $\partial\mathcal{B}$ for the surface tractions and couples, respectively represented by the vector $\mathbf{t}$ and the skew–symmetric tensor $\mathbf{C}$ ($\mathbf{C} = -\mathbf{C}^T$), are:

$$\begin{aligned} \mathbf{S}\,\mathbf{n} &= \mathbf{t}, \\ \mathbb{S}\,\mathbf{n} &= \mathbf{C}, \end{aligned} \tag{19}$$

$\mathbf{n}$ being the outward normal to the boundary $\partial\mathcal{B}$.

The stress–strain relations for the linear elastic anisotropic micropolar material can be written:

$$\begin{aligned} \mathbf{S} &= \underline{\mathbb{A}}\,\mathbf{U} + \underline{\mathbb{B}}\,\mathbb{U}, \\ \mathbb{S} &= \underline{\mathbb{C}}\,\mathbf{U} + \underline{\mathbb{D}}\,\mathbb{U}, \end{aligned} \tag{20}$$

where $\underline{\mathbb{A}}$ and $\underline{\mathbb{D}}$ are fourth, and sixth order constitutive tensors with the major symmetries, respectively, while $\underline{\mathbb{B}}$ and $\underline{\mathbb{C}}$, are fifth order constitutive tensors respecting the symmetry relation: $\underline{\mathbb{B}}\mathbb{V}\cdot\mathbf{V} = \underline{\mathbb{C}}\mathbf{V}\cdot\mathbb{V}$, $\forall\mathbf{V},\mathbb{V}$. It is worth noting that in the presence of central symmetries, the tensors $\underline{\mathbb{B}}$ and $\underline{\mathbb{C}}$ are null and Equations (20) reduce to:

$$\begin{aligned} \mathbf{S} &= \underline{\mathbb{A}}\mathbf{U}, \\ \mathbb{S} &= \underline{\mathbb{D}}\mathbb{U}. \end{aligned} \tag{21}$$

Taking into account the decomposition in the symmetric and skew–symmetric part of the stress and strain tensors, Equations (21) can be also written:

$$\begin{aligned} \mathbf{T} &= \underline{\mathbb{A}}^{YY}\mathbf{E} + \underline{\mathbb{A}}^{YK}(\boldsymbol{\Theta} - \mathbf{W}), \\ \mathbf{A} &= \underline{\mathbb{A}}^{KY}\mathbf{E} + \underline{\mathbb{A}}^{KK}(\boldsymbol{\Theta} - \mathbf{W}), \\ \mathbb{S} &= \underline{\mathbb{D}}\,\mathbb{U}, \end{aligned} \tag{22}$$

where the constitutive tensors $\underline{\mathbb{A}}^{\alpha\beta}$ ($\alpha, \beta = Y, K$) have components obtained as linear combination of the components of the constitutive tensors in (21).

3.2. The meso–level micropolar model

The constitutive equations for the meso–level two–phase elastic materials (inclusions and matrix) are identified, using Equations (14, 15), in the general anisotropic form (20), which specialize in the form (21) or (22) in the case of central symmetry.

Let us now consider a two–dimensional portion of the reference material, in the case in which the result of the coarse–graining procedure identifies two linear elastic (micropolar) isotropic phases. By reordering into vectors the components of the symmetric and skew–symmetric stress ($\mathbf{T}$, $\mathbf{A}$) since and strain ($\mathbf{E}$, $\boldsymbol{\Theta}$) tensors, together with the sole independent

components of the couple–stress $\mathbb{S}$ (denoted as $\mathbf{s}_1$, $\mathbf{s}_2$) and curvature $\mathbb{U}$ (denoted as $\mathbf{u}_1$, $\mathbf{u}_2$) tensors, the constitutive equations can be written as:

$$\begin{bmatrix} \mathbf{T}_{11} \\ \mathbf{T}_{22} \\ \mathbf{T}_{12} \\ \mathbf{A}_{12} \\ \mathbf{s}_1 \\ \mathbf{s}_2 \end{bmatrix} = \begin{bmatrix} \lambda+2\mu & \lambda & 0 & 0 & 0 & 0 \\ \lambda & \lambda+2\mu & 0 & 0 & 0 & 0 \\ 0 & 0 & 2\mu & 0 & 0 & 0 \\ 0 & 0 & 0 & -2\mu_c & 0 & 0 \\ 0 & 0 & 0 & 0 & 2\mu l_c^2 & 0 \\ 0 & 0 & 0 & 0 & 0 & 2\mu l_c^2 \end{bmatrix} \begin{bmatrix} \mathbf{E}_{11} \\ \mathbf{E}_{22} \\ \mathbf{E}_{12} \\ \boldsymbol{\Theta}_{12} - \mathbf{W}_{12} \\ \mathbf{u}_1 \\ \mathbf{u}_2 \end{bmatrix}, \tag{23}$$

given that any second order tensor, $\mathbf{V}$, has components defined as: $\mathbf{V}_{ij} = \mathbf{V} \cdot \mathbf{e}_i \otimes \mathbf{e}_j$ (where $\{\mathbf{e}_i, \mathbf{e}_j\}$, $i, j = 1, 2$, defines an orthonormal base for the two-dimensional space).

Equations (23) show that the non–null constitutive tensors $\underline{\mathbb{A}}$ and $\underline{\mathbb{D}}$ in (21) have components depending on four independent elastic constitutive parameters: the Lamé constants λ and μ, the Cosserat shear modulus μ_c, and the so–called characteristic length l_c, which is responsible for the bending stiffness. These parameters are those resulting from the identification procedure of Section 2 applied to the the case of our reference material (Figure 3), as it will be described in Section 4.

3.3. The macro-level micropolar model

The effective elastic components of the micropolar macro–level continuum are directly obtained from the homogenization procedure, consistent with a properly defined generalized macrohomogeneity condition, which establishes an energetic equivalence between a portion of the heterogeneous material at the mesoscopic level and the material point at the macroscopic level.

In this respect, let us now consider a representative portion of the heterogeneous material at the meso–scale, i.e. a region $\mathcal{B}_\delta$ of volume V_δ and size L (where $\delta = L/d$ is the scale factor, with d being the average inclusion size). By taking into account the splitting into symmetric and skew–symmetric strain and stress components the generalized macrohomogeneity condition writes:

$$\overline{\mathbf{T} \cdot \mathbf{E}} + \overline{\mathbf{A} \cdot (\boldsymbol{\Theta} - \mathbf{W})} + \frac{1}{2}\,\overline{\mathbb{S} \cdot \mathbb{U}} = \frac{1}{V_\delta} \int_{\mathcal{B}_\delta} (\mathbf{T} \cdot \mathbf{E} + \mathbf{A} \cdot (\boldsymbol{\Theta} - \mathbf{W}) + \frac{1}{2}\,\mathbb{S} \cdot \mathbb{U})\, dV\,, \tag{24}$$

where overbars denote macroscopic quantities obtained as volume averages of the corresponding mesoscopic variables, i.e.: $\overline{(\cdot)} = \frac{1}{V_\delta} \int_{\mathcal{B}_\delta} (\cdot)\, dV$.

The generalized macrohomogeneity condition (24) requires that the power expended by the stress in the strain at the mesoscopic level equals the power of the stress at the macroscopic level. As the meso– and the macro–model are both micropolar continua, this condition ensures a one–to–one correspondence between the two scales, avoiding the

introduction of kind of internal constraints for the deformation mechanisms, as occurs when continua of different type are connected [14]. The condition is verified providing that the following BCS hold.
- Dirichlet's boundary conditions (D–BC):

$$\begin{aligned} &\mathbf{w}\,|_{\partial\mathcal{B}} = \overline{\mathbf{E}}\,\mathbf{x}, \\ &\mathbf{\Theta}\,|_{\partial\mathcal{B}} = \overline{\mathbf{\Theta}} - \overline{\mathbf{W}}\,, \qquad \mathbf{W}|_{\partial\mathcal{B}} = \overline{\mathbb{U}}\,\mathbf{x}\,. \end{aligned} \tag{24}$$

where $\mathbf{x}$ is the position vector of a point on boundary. Alternatively:
- Neumann's boundary conditions (N–BC):

$$\begin{aligned} &\mathbf{T}\,\mathbf{n}\,|_{\partial\mathcal{B}} = \overline{\mathbf{T}}\,\mathbf{n}\,, \\ &\mathbb{S}\,\mathbf{n}\,|_{\partial\mathcal{B}} = \frac{1}{2}[(\mathbf{x}\otimes\mathbf{A}\,\mathbf{n} - \mathbf{A}\,\mathbf{n}\otimes\mathbf{x}) + \overline{\mathbb{S}}\,\mathbf{n}]\,. \end{aligned} \tag{24}$$

Consistently with the above, the effective macroscopic stress–strain relations result in the (in general anisotropic) form:

$$\begin{aligned} \overline{\mathbf{S}} &= \underline{\overline{\mathbb{A}}}\ \overline{\mathbf{U}} + \underline{\overline{\mathbb{B}}}\ \overline{\mathbb{U}}, \\ \overline{\mathbb{S}} &= \underline{\overline{\mathbb{C}}}\ \overline{\mathbf{U}} + \underline{\overline{\mathbb{D}}}\ \overline{\mathbb{U}}, \end{aligned} \tag{24}$$

Considering two–dimensional assemblies for which the central symmetry holds, we have $\mathbb{B} = \mathbb{C} = \mathsf{0}$, and the constitutive equations, and taking into account the decomposition into symmetric and skew–symmetric parts of the stress and strain tensors, can be written as:

$$\begin{aligned} \overline{\mathbf{T}} &= \underline{\overline{\mathbb{A}}}^{YY}\overline{\mathbf{E}} + \underline{\overline{\mathbb{A}}}^{YK}(\overline{\mathbf{\Theta}} - \overline{\mathbf{W}}), \\ \overline{\mathbf{A}} &= \underline{\overline{\mathbb{A}}}^{KY}\overline{\mathbf{E}} + \underline{\overline{\mathbb{A}}}^{KK}(\overline{\mathbf{\Theta}} - \overline{\mathbf{W}}), \\ \bar{\mathbf{s}} &= \underline{\overline{\mathbf{D}}}\,\bar{\mathbf{u}}\,, \end{aligned} \tag{23}$$

The independent strain and stress components of the stress and strain tensors can be conveniently ordered into vectors, and considering the Voigt notation derived as described above, Equations (23) specialize in:

$$\begin{bmatrix} \overline{\mathbf{T}}_{11} \\ \overline{\mathbf{T}}_{22} \\ \overline{\mathbf{T}}_{12} \\ \overline{\mathbf{A}}_{12} \\ \bar{\mathbf{s}}_1 \\ \bar{\mathbf{s}}_2 \end{bmatrix} = \begin{bmatrix} \underline{\overline{\mathbb{A}}}^{YY}_{1111} & \underline{\overline{\mathbb{A}}}^{YY}_{1122} & \underline{\overline{\mathbb{A}}}^{YY}_{1112} & \underline{\overline{\mathbb{A}}}^{YK}_{1121} & 0 & 0 \\ \underline{\overline{\mathbb{A}}}^{YY}_{2211} & \underline{\overline{\mathbb{A}}}^{YY}_{2222} & \underline{\overline{\mathbb{A}}}^{YY}_{2212} & \underline{\overline{\mathbb{A}}}^{YK}_{2221} & 0 & 0 \\ \underline{\overline{\mathbb{A}}}^{YK}_{1211} & \underline{\overline{\mathbb{A}}}^{YK}_{1222} & \underline{\overline{\mathbb{A}}}^{YK}_{1212} & \underline{\overline{\mathbb{A}}}^{YK}_{1221} & 0 & 0 \\ \underline{\overline{\mathbb{A}}}^{KY}_{1211} & \underline{\overline{\mathbb{A}}}^{KY}_{1222} & \underline{\overline{\mathbb{A}}}^{KY}_{1212} & \underline{\overline{\mathbb{A}}}^{KK}_{1212} & 0 & 0 \\ 0 & 0 & 0 & 0 & \underline{\overline{\mathbf{D}}}_{11} & \underline{\overline{\mathbf{D}}}_{22} \\ 0 & 0 & 0 & 0 & \underline{\overline{\mathbf{D}}}_{21} & \underline{\overline{\mathbf{D}}}_{22} \end{bmatrix} \begin{bmatrix} \overline{\mathbf{E}}_{11} \\ \overline{\mathbf{E}}_{22} \\ \overline{\mathbf{E}}_{12} \\ \overline{\mathbf{\Theta}}_{12} - \overline{\mathbf{W}}_{12} \\ \bar{\mathbf{u}}_1 \\ \bar{\mathbf{u}}_2 \end{bmatrix} \tag{24}$$

The components of the constitutive tensors in Equation (24) are expressed as linear combination of the components of the tensors in (24), which in the special case of orthotropy coincide with the ones of Equation (28) in [53]. The components of any tensors $\mathbb{V}$, of order N, in (24) are defined as: $\mathbb{V}_{ij...N} = \mathbb{V} \cdot (\mathbf{e}_i \otimes \mathbf{e}_j, ..., \otimes \mathbf{e}_N)$, $\{\mathbf{e}_i, \mathbf{e}_j, ..., \mathbf{e}_N\}$ $(i, j, ..., N = 1, 2)$ being an orthonormal base of size N.

4. Numerical simulations

In the exemplifying case study here presented, the material is characterized by particles randomly arranged into a base matrix, either stiffer, case (a), named higher contrast material, or softer, case (b), named lower contrast material; where the term contrast refers to the ratio between elastic moduli of inclusions and matrix.

The three–scale procedure described in Sections 2 and 3 has been implemented and adopted to evaluate the equivalent micropolar elastic response of a two–dimensional, ideally homogeneous, material that qualitatively mimics the internal microstructure of a Ceramic Matrix Composite, as the Alumina-Zirconia qualitatively described in Section 1.

Going from the micro– up to the meso– and then the macro–scale, the material is described as follows. At the micro–scale the microstructure, of both matrix and inclusions, is made of a periodic assemblage of hexagonal rigid particles, regularly arranged and connected by axial, translational and rotational springs. This assumption certainly represents a simplification in the detailed description of polycristalline microstructures in which the porosity, as well as development of local plasticity and internal microdefects during loading can play important roles [46, 54, 55, 56]. With this microscopic model, however, the overall elastic, possibly isotropic, behavior of kinds of microstructures, high volume fraction as CMC of Figure 2, can be derived resorting to a limited set of parameters, i.e. the stiffness of the springs, that via energy equivalence criteria can properly calibrate the elasticities of the microscopic level (topologies different from the hexagonal one are needed in the case of anisotropy, as for instance in the orthotropic assemblies of [53]).

In Figure 4 a schematic of a periodic cell (module), that can be representative both of the matrix and of the inclusions, is shown: each cell is a hexagon, surrounded by six hexagons interacting through six 'test pairs' (black circles, represented by springs located at the center of each side of the hexagons). It is worth noting that this illustrative example is not directly related to a specific material; it represents the ideal material that qualitatively mimics CMC with high volume fraction of nearly hexagonal particles.

The micro/meso transition (i), described in Section 2, is thus performed by respectively adopting for the two phases, matrix and inclusions, the geometric and mechanical parameters shown in Table 1; where l_μ is the side length of the rigid hexagonal block, $\mathbf{K}_p$ is the stiffness tensor in Equation (7a), collecting the axial and shear stiffness of the springs, while $(\mathbb{K}_p)$ is the sole independent component of the stiffness tensor in (7b), i.e. the rotational

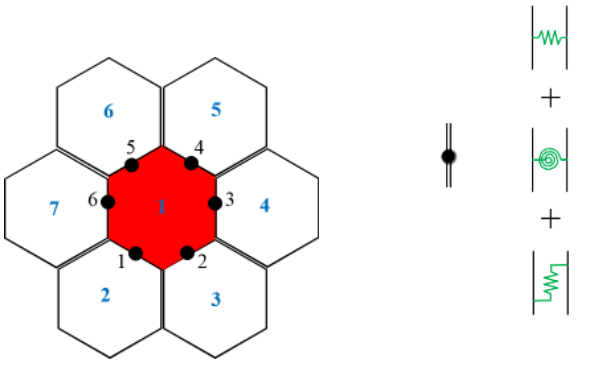

(a) (b)

Figure 4: (a) Hexagonal periodic cell: assemblage of rigid particles connected by point–like springs;(b) Schematic of the contact ('test pair'): axial; rotational; translational spring.

(a)matrix/(b)inclusions	$l_\mu = 7$	$(\mathbf{K}_p) = \begin{pmatrix} 2000 & 0 \\ 0 & 3450 \end{pmatrix}$; $(\mathbb{K}_p) = 6125$
(a)inclusions/(b)matrix	$l_\mu = 0.6$	$(\mathbf{K}_p) = \begin{pmatrix} 785 & 0 \\ 0 & 780 \end{pmatrix}$; $(\mathbb{K}_p) = 17.66$

Table 1: Geometric and elastic coefficients of the interfaces. l_μ is the side length of the rigid hexagonal block, $\mathbf{K}_p$ collects the axial and shear stiffness of the springs and $(\mathbb{K}_p)$ is the rotational stiffness of the spring.

stiffness of the spring. In this way it is possible to gather information related to micropolar moduli, usually very difficult to measure in experimental tests, directly from the inner microstructure of the polycristalline material. One of the advantages of this three steps procedure, that moves from a physically–based discrete description at the micro–level, is that, on the tracks of the classical molecular theory of elasticity [40], we can rationally derive the micropolar constants generally difficult to obtain resorting to standard experimental results [52]. As our aim is to explain the identification procedure, all the parameters describing the spring stiffness are assumed known and expressed in dimensionless form.

For the two phases, the result of the coarse–graining process is an isotropic materials with the elastic coefficients expressed in Equation (23). These homogenized values are then adopted as material parameters at the mesoscopic level. In particular, our interest is here restricted to the evaluation of the Cosserat shear modulus μ_c and the bending modulus related to the characteristic length l_c. The results of the coarse–graining (first–step) procedure are expressed in terms of material contrasts (i.e. the ratio between the inclusions and matrix constants), focusing on Cosserat shear and bending moduli. The identified ratios between

the micropolar constants of inclusions and matrix (non–standard material contrast) for the material (a) are: $\mu_i/\mu_m = 4.93$ and $l_{c_i}/l_{c_m} = 10$, while for the material (b), in which the parameters of matrix and inclusions are exchanged, are: $\mu_i/\mu_m = 0.202$ and $l_{c_i}/l_{c_m} = 0.1$. For the chosen module with elastic coefficient of Table 1, the derived constitutive coefficients of the matrix in (23) are strictly diagonal and, as a consequence, no Poisson's effects are accounted for. However, more general assumptions are possible [3], also by resorting to multiple interactions [57]. Adopting this three steps procedure, that moves from a physically–based discrete description at the micro–level on the tracks of [40], we can rationally derive the multifield continua parameters, focusing on the micropolar constants that are generally difficult to obtain resorting to standard experimental results.

The meso/macro homogenization (ii) of Section 3 is then carried out, in turn. We exploit the statistically–based multi–scale procedure, developed and detailed in [33], in order to achieve the twofold purpose of detecting the RVE size, L_{RVE}, and estimating the constitutive moduli of the energy equivalent homogeneous micropolar continuum.

Briefly, by fixing some parameters (as: inclusions density; size, d; shape and the material parameters of constituents obtained at the step (i)) and randomly varying other parameters, as the number and position of the particles, under hypotheses of statistical homogeneity and mean ergodicity, the solution of series of Boundary Value Problems (BVPs) on representative square regions $\mathcal{B}_\delta$ of size L, called Statistical Volume Elements (SVEs), is obtained using a so–called moving window technique. The windows are chosen in such a way that their edges randomly intersect the particles. Then, by varying the scale factor $\delta = L/d$ and by solving both the Dirichlet and Neumann BVPs for all the random representations of the internal structure $\mathcal{B}_\delta(\omega)$, ω being an elementary event over a sample space (a frozen moving window, namely the SVE), the procedure provides hierarchies of bounds for the elastic coefficients that allow us to estimate of the size of the RVE for performing homogenization. The convergence to the RVE is ensured by a statistical criterion of convergence specifically defined. This criterion allow us to stop the procedure when the number of simulations, necessary to obtain averages of elastic coefficients that do not differ from a given tolerance, is small enough (where the interval is evaluated at 95% over a normal standard distribution).

With regard to the reference material here considered, we can observe that this also exhibits, at the macroscopic level, a nearly isotropic homogenized behavior. In this case the micropolar shear stress, $\overline{\mathbf{A}}_{12}$, is a scalar term related to the relative rotation, $(\overline{\mathbf{\Theta}}_{12} - \overline{\mathbf{W}}_{12})$, through the constitutive component $\underline{\overline{\mathbb{A}}}^{KK}_{1212}$, while the couple stress, $\bar{\mathbf{s}}$, and the curvature, $\overline{\mathbf{u}}$, are related through the modulus $\mathrm{tr}\underline{\overline{\mathbf{D}}}$; thus the following relations hold:

$$\begin{aligned} \overline{\mathbf{A}}_{12} &= \underline{\overline{\mathbb{A}}}^{KK}_{1212}\,(\overline{\mathbf{\Theta}}_{12} - \overline{\mathbf{W}}_{12}) \\ \{\bar{\mathbf{s}}\} &= \frac{1}{2}\,\mathrm{tr}\,\underline{\overline{\mathbf{D}}}\{\overline{\mathbf{u}}\}\,, \end{aligned} \tag{24}$$

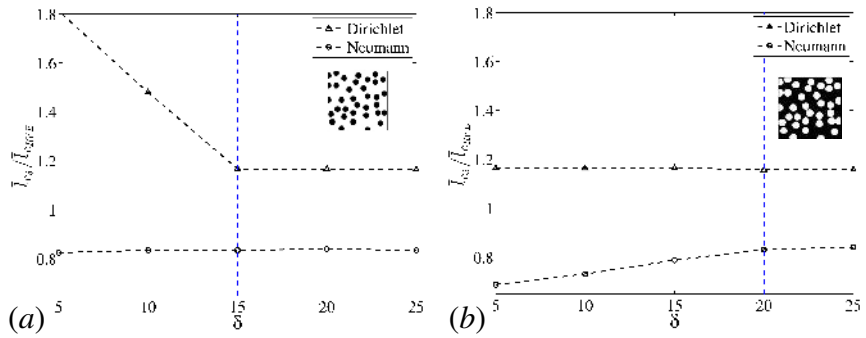

Figure 5: Effective bending modulus $\bar{l}_c$ (normalized to the RVE modulus $\bar{l}_{cRVE}$) versus scale parameter δ obtained under Dirichlet-BC and Neumann-BC. (a): inclusion stiffer than the matrix ; (b): inclusion softer than the matrix. (Dashed line at δ_{REV}).

where these equations are extracted from (24), which in this isotropic case specialize with the components: $\underline{\overline{\mathbb{A}}}^{YY}_{1111} = \underline{\overline{\mathbb{A}}}^{YY}_{2222} = \overline{\lambda} + 2\,\overline{\mu}$, $\underline{\overline{\mathbb{A}}}^{YY}_{1122} = \underline{\overline{\mathbb{A}}}^{YY}_{2211} = \overline{\lambda}$, $\underline{\overline{\mathbb{A}}}^{YY}_{1212} = 2\,\overline{\mu}$, $\underline{\overline{\mathbb{A}}}^{KK}_{1212} = 2\,\overline{\mu}_c$, $\underline{\overline{\mathbf{D}}}_{11} = \underline{\overline{\mathbf{D}}}_{22} = 2\,\overline{\mu_c\, l_c^2}$, while all the other constitutive components being null.

We then consider the modulus $\overline{l_c} = \sqrt{\mathrm{tr}\,\underline{\overline{\mathbf{D}}}/\underline{\overline{\mathbb{A}}}^{KK}_{1212}}$, related to the micropolar bending and shear stiffness, for representing the convergence trend to the RVE of the micropolar material response obtained by varying the scale ratio δ, while maintaining the inclusion size d constant. This modulus represents the characteristic internal length of the micropolar continuum, and allow us to focuses on the main peculiarity of this multifield model, that is to account of the size and the stress and strain skew–symmetric effects.

In Figure 5a the average of the characteristic length $\overline{l_{c\delta}}$ versus the scale parameter δ, normalized with respect to the RVE value $\overline{l_{cRVE}}$, is reported for the material (a). Solutions of both boundary value problems under Dirichlet and Neumann boundary conditions are plotted. The adopted convergence criterion indicates that the RVE is achieved for $\delta_{RVE} = 15$. Analogously, in Figure 5b the same normalized bending modulus $\overline{l_{c\delta}}$ versus δ is shown for material (b). In this case the size of the RVE corresponds to a higher value of δ_{RVE} ($\delta_{RVE} = 20$). The different contrasts between material parameters characterizing materials (a) and (b) influence the convergence trend of the constitutive parameters, as the dimension L of the SVE increases. The material (b) shows a slower convergence than material (a), nevertheless the occurrence of horizontal plateau indicates that, independently on the material contrast, the RVE is reached and that the corresponding homogenized modulus is obtainable as the average value between the Dirichlet and Neumann solutions.

5. Final remarks

We have developed a multi–scale homogenization approach for the study of composite materials characterized by microstructural length scales not negligible with respect to the

mesoscopic and macroscopic characteristic lengths. The proposed procedure is able to describe the material behavior following a complete hierarchy of scales from the microscopic up to the macroscopic scale.

The material is modeled at three levels. The micro–level, characterized by the length scale l_μ, where each constituent is described as a modular discrete system; at this level, even if this is not a necessary option, the material is supposed deterministic, due to the high volume fraction of the material (high concentration of particles) or to the actual regularity of the microstructure. The meso–level, where a material sample of length L is considered and modeled as a two–phases micropolar material made of inclusions of size d randomly embedded in a matrix. The macro–level, characterized by structural length L_M, where an equivalent homogeneous micropolar material is obtained as final result of the multi–scale procedure.

The micro/meso transition is performed via a coarse–graining procedure based on a generalized Cauchy–Born correspondence map and energy equivalence between the microscopic periodic lattice system, describing each material constituent, and the equivalent micropolar material. For the meso/macro transition, instead, a statistical homogenization procedure has been developed, basing on the solution of boundary value problems posed on statistically representative elements, under boundary conditions derived from a generalized macrohomogeneity condition of Hill's type. The paper extends two approaches previously independently developed [51], [33] and here organically combined into an integrated multiscale approach.

An illustrative numerical example is finally provided to assess the capabilities of the procedure. An ideal material that mimics the internal microstructure of a ceramic matrix composite is studied starting from its hexagonal discrete microstructure. At the mesoscopic scale the random nature of the material is taken into account and the overall homogenized macroscopic micropolar elastic moduli are finally obtained. We showed that the micro–level description allow us to derive the micropolar elastic moduli that cannot be detected using standard experimental equipments.

This procedure provides an appropriate base framework for future investigation of the non–linear behavior of microstructured materials. We expect that the multiscale paradigm allow us to describe the occurrence of damage/fracture phenomena at the micro–scale [46], and then, by exchanging information with the coarser scales, to obtain the non-linear effective/macroscopic response of the micropolar continuum taking into account the size and spatial random distribution of particles, as successfully done for regular masonry [10].

Acknowledgement

The author gratefully acknowledges support from MIUR Prin National Grant 2015; Sapienza University Grant 2016.

References

[1] Luciano Feo, Fernando Fraternali, and Robert E. Skelton. Special issue on composite lattices and multiscale innovative materials and structures. *Composites Part B: Engineering*, 2006.

[2] S. Forest and K. Sab. Cosserat overall modeling of heterogeneous materials. *Mechanics Research Communications*, 25:449–454, 1998.

[3] R. Masiani and P. Trovalusci. Cosserat and Cauchy materials as continuum models of brick masonry. *Meccanica*, 31:421–432, 1996.

[4] O. van der Sluis, P. H. J. Vosbeek, P. J. G. Schreurs, and H. E. H. Meijer. Homogenization of heterogeneous polymers. *International Journal of Solids and Structures*, 36:3193–3214, 1999.

[5] S. Forest, R. Dendievel, and G. R. Canova. Estimating the overall properties of heterogeneous Cosserat materials. *Modelling and Simulation in Materials Science and Engineering*, 7:829–840, 1999.

[6] R. Luciano and J. R. Willis. Bounds on non-local effective relations for random composites loaded by configuration-dependent body force. *Journal of the Mechanics and Physics of Solids*, 48(9):1827 – 1849, 2000.

[7] P. Onck. Cosserat modeling of cellular solids. *Comptes Rendus Mecanique*, 330:717–722, 2002.

[8] V. G. Kouznetsova, M. G. D. Geers, and W. A. M. Brekelmans. Multi-scale constitutive modelling of heterogeneous materials with a gradient-enhanced computational homogenization scheme. *International Journal for Numerical Methods in Engineering*, 54:1235–1260, 2002.

[9] P. Trovalusci and G. Augusti. A continuum model with microstructure for materials with flaws and inclusions. *Journal de Physique IV*, Pr8:383–390, 1998.

[10] P. Trovalusci and R. Masiani. Non-linear micropolar and classical continua for anisotropic discontinuous materials. *International Journal of Solids and Structures*, 40:1281–1297, 2003.

[11] R. Larsson and S. Diebels. A second-order homogenization procedure for multi-scale analysis based on micropolar kinematics. *International Journal for Numerical Methods in Engineering*, 69:2485–2512, 2007.

[12] Xi Yuan, Yoshihiro Tomita, and Tomoaki Andou. A micromechanical approach of nonlocal modeling for media with periodic microstructures. *Mechanics Research Communications*, 35(1–2):126 – 133, 2008.

[13] P. Trovalusci, V. Varano, and G. Rega. A generalized continuum formulation for composite materials and wave propagation in a microcracked bar. *Journal of Applied Mechanics*, 77(6):061002–1/11, 2010.

[14] M. L. De Bellis and D. Addessi. A Cosserat based multi-scale model for masonry structures. *International Journal of Multiscale Computational Engineering*, 9(5):543–563, 2011.

[15] S. Forest and D. K. Trinh. Generalised continua and the mechanics of heterogeneous material. *Zeitschrift für Angewandte Mathematik und Mechanik*, 91:90–109, 2011.

[16] P. Trovalusci and A. Pau. Derivation of microstructured continua from lattice systems via principle of virtual works. The case of masonry-like materials as micropolar, second gradient and classical continua. *Acta Mechanica*, 225(1):157–177, 2014.

[17] Daniela Addessi, Maria Laura De Bellis, and Elio Sacco. A micromechanical approach for the cosserat modeling of composites. *Meccanica*, 51(3):569–592, 2016.

[18] L. Barretta R., Feo, Luciano R., and F. Marotti de Sciarra. An Eringen-like model for Timoshenko nanobeams. *Composite Structures*, 139:104 – 110, 2016.

[19] P. Trovalusci. Molecular approaches for multifield continua: origins and current developments. In T. Sadowsky and P. Trovalusci, editors, *Multiscale Modelling of Complex Materials: phenomenological, theoretical and computational aspects*, number 556 in CISM Courses and Lectures, pages 211–278. Springer, Berlin, 2014.

[20] P. Trovalusci. *Materials with Internal Structure. Multiscale and Multifield Modeling and Simulation*. Springer, Berlin, 2016.

[21] H. Altenbach and V. A. Eremeyev, editors. *Generalized Continua as Models for Classical and Advanced Materials*, volume 42 of *Advanced Structured Materials*. Springer, Berlin, 2016.

[22] L. J. Sluys, R. de Borst, and H. B. Mühlhaus. Wave propagation, localization and dispersion in a gradient-dependent medium. *International Journal of Solids and Structures*, 30:1153–1171, 1993.

[23] G. A. Maugin. Nonlocal theories or gradient–type theories: a matter of convenience? *Archives of Mechanics*, 31(1):15–26, 1979.

[24] Isaak Abramovich Kunin. *Elastic media with microstructure I: one-dimensional models*, volume 26. Springer Verlag, Berlin, 1982. Original Russian edition 1975.

[25] A. C. Eringen. Mechanics of micromorphic materials. In *Proc. 11th Int. Congress of Applied Mechanics*, pages 131–138. Springer–Verlag, 1964.

[26] W. Nowacki, editor. *Theory of Micropolar Elasticity*, volume 25 of *International Centre for Mechanical Sciences, Courses and Lectures*. Springer–Verlag, Berlin, 1970.

[27] G. Capriz. *Continua with Microstructure*. Springer-Verlag, Berlin, 1989.

[28] J. Altenbach, H. Altenbach, and V. A. Eremeyev. On generalized Cosserat-type theories of plates and shells:a short review and bibliography. *Archives of Applied Mechanis*, 80:73–92, 2010.

[29] H. Altenbach and V. A. Eremeyev, editors. *Generalized Continua from the Theory to Engineering Application*, volume 541 of *CISM Courses and Lectures*. Springer, Berlin, 2013.

[30] V. A. Eremeyev and W. Pietraszkiewicz. Material symmetry group and constitutive equations of micropolar anisotropic elastic solids. *Mathematics and Mechanics of Solids*, pages 1–12, 2015.

[31] F. Dos Reis and J.-F. Ganghoffer. Construction of micropolar continua from the homogenization of repetitive planar lattices. In H. Altenbach, G. A. Maugin, and V. Erofeev, editors, *Mechanics of Generalized Continua*, number 7 in Advanced Structured Materials, pages 193–217, Berlin Heidelberg, 2011. Springer–Verlag.

[32] F. Dos Reis and J.-F. Ganghoffer. Construction of micropolar continua from the asymptotic homogenization of beam lattices. *Computers and Structures*, 112–113:354–363, 2012.

[33] P. Trovalusci, M. Ostoja-Starzewski, M. L. De Bellis, and A. Murrali. Scale–dependent homogenization of random composites as micropolar continua. *European Journal of Mechanics A/Solids*, 49:396–407, 2015.

[34] P. Trovalusci, M. Ostoja-Starzewski, M. L. De Bellis, and A. Murrali. Particulate random composites homogenized as micropolar materials. *Meccanica*, 49(9):2719–2727, 2015.

[35] M. Ostoja-Starzewski. Macrohomogeneity condition in dynamics of micropolar media. *Archive of Applied Mechanics*, 81:899–906, 2011.

[36] V. Naglieri, P. Palmero, L. Montanaro, and J. Chevalier. Elaboration of alumina-zirconia composites: Role of the zirconia content on the microstructure and mechanical properties. *Materials*, 6:2090–2102, 2013.

[37] Carlos A. Fortulan and Dulcina P.F. de Souza. Microstructural evolution of the $Al_2 2O_3$-ZrO_2 composite and its correlation with electrical conductivity. *Materials Research*, 2:205 – 210, 1999.

[38] P. Trovalusci, D. Capecchi, and G. Ruta. Genesis of the multiscale approach for materials with microstructure. *Archive of Applied Mechanics*, 79:981–997, 2009.

[39] D. Capecchi, G. Ruta, and P. Trovalusci. From classical to Voigt's molecular models in elasticity. *Archive for History of Exact Sciences*, 64:525–559, 2010.

[40] J. L. Ericksen. Special topics in elastostatics. In C. S. Yih, editor, *Advances in Applied Mechanics*, volume 17, pages 189–244. Academic Press, New York, 1977.

[41] A. Di Carlo, N. Rizzi, and A. Tatone. Continuum modelling of beam-like latticed truss: Identification of the constitutive functions for the contact and inertial actions. *Meccanica*, 25(3):168–174, 1990.

[42] Geminiano Mancusi, Francesco Fabbrocino, Luciano Feo, and Fernando Fraternali. Size effect and dynamic properties of 2D lattice materials. *Composites Part B: Engineering,*, 112:235–242, 2016.

[43] R. Barretta, R. Luciano, and J. R. Willis. On torsion of random composite beams. *Composite Structures*, 132:915 – 922, 2015.

[44] M. Ostoja-Starzewski. Material spatial randomness: From statistical to representative volume element. *Probabilistic Engineering Mechanics*, 21:112–132, 2006.

[45] Z. Khisaeva and M. Ostoja-Starzewski. On the size of RVE in finite elasticity of random composites. *Journal of Elasticity*, 85:153–173, 2006.

[46] T. Sadowski and L. Marsavina. Multiscale modelling of two-phase ceramic matrix composites. *Computational Materials Science*, 50(4):1336 – 1346, 2011.

[47] Fabrizio Greco, Lorenzo Leonetti, Raimondo Luciano, and Paolo Nevone Blasi. An adaptive multiscale strategy for the damage analysis of masonry modeled as a composite material. *Composite Structures*, 153:972–988, 2016.

[48] D. Besdo. Inelastic behaviour of plain frictionless block-systems described by Cosserat media. *Archives of Mechanics*, 37:603–619, 1985.

[49] H. B. Mühlhaus. Application of cosserat theory in numerical solutions of limit load problems. *Ingenieur-Archiv*, 59(2):124–137, 1989.

[50] S. C. Chang and C. Liao. Constitutive relation for a particulate medium with the effect of particle rotation. *International Journal of Solids and Structures*, 26(4):437–453, 1990.

[51] P. Trovalusci and R. Masiani. Material symmetries of micropolar continua equivalent to lattices. *International Journal of Solids and Structures*, 36(14):2091–2108, 1999.

[52] R Lakes. Experimental micro mechanics methods for conventional and negative Poisson's ratio cellular solids as Cosserat continua. *Journal of Engineering Materials and Technology*, 113(1):148–155, 1991.

[53] A. Pau and P. Trovalusci. Block masonry as equivalent micropolar continua: the role of relative rotations. *Acta Mechanica*, 223(7):1455–1471, 2012.

[54] E. Postek and T. Sadowski. Assessing the influence of porosity in the deformation of metal–ceramic composites. *Composite Interfaces*, 18(1):57–76, 2011.

[55] Gradual degradation in two–phase ceramic composites under compression. *Computational Materials Science*, 64:209 – 211, 2012.

[56] T. Sadowski and B. Pankowski. Numerical modelling of two-phase ceramic composite response under uniaxial loading. *Composite Structures*, 143:388 – 394, 2016.

[57] D. Capecchi, G. Ruta, and P. Trovalusci. Voigt and Poincaré's mechanistic–energetic approaches to linear elasticity and suggestions for multiscale modelling. *Archive of Applied Mechanics*, 81(11):1573–1584, 2011.